Estimation of Degree of Polarization in Low Light Using Truncated Poisson Distribution

Marcos Aviñoá, Xin Shen, *Member, IEEE*, Salvador Bosch, Bahram Javidi, *Fellow, IEEE*, and Artur Carnicer

***Abstract*—The Degree of Polarization (DoP) of a light beam inside a medium contains unique information about the medium. 3D imaging techniques constitute an optimal procedure for determining the DoP under low light conditions, as the computational reconstruction process can increase the signal-to-noise ratio of the detected light. The definition of the DoP contains a division by the total number of detected photons from the sensor. However, under photon starved conditions, the number of detected photons at a single time period may be equal to zero. This may pose a division by zero problem for the computation of DoP. In this work, we consider a truncated Poisson distribution to overcome this problem and show that the mean value of the computed DoP goes to zero independently of the state of polarization of the light. The validity of our approach is verified by capturing the light fields of a test object to compute its DoP under low light conditions. The formulae derived in this work can be used to correct the deviation of the mean value of the DoP with respect to the ideal measurements.**

***Index Terms*—Optical imaging, optical physics, optical polarization, stokes parameters.**

I. Introduction

THE vector nature of light and its phase information are two fascinating quantities, as well as elusive ones. The former can provide information about the properties of the material from the light reflected or generated from the material surface; the latter provides information related to the curvature of the wavefront and its propagation. Unfortunately, in the detection process, we will lose all the information in respect to the aspects mentioned above, because photodetectors are only sensitive to the number of photons incident on the sensor. [1], [2].

Polarimetric imaging is an image-detection technique which allows for the detection of the vector properties of light and its polarization state [3]. One of the most interesting values obtained from these measurements is the Degree of Polarization (DoP). DoP is a number between zero and one, which indicates the ratio of polarized light with respect to the total amount of light in the beam. Theoretically, this measurement is independent of the amount of light emitted or reflected from a material surface, and it can be very useful for the object recognition and material classification in a scene [4]–[7].

Part of the information about the propagation of light can be recovered using a 3D imaging technology initially proposed by Lippmann [8], called Integral Imaging. In this approach, not only the light irradiance is captured, but also the direction that the light rays had upon arriving at the camera. A conventional Integral Imaging capture system consists of a planar array of traditional cameras [9]. This imaging technology has been extensively exploited to improve the detection of DoP [10]–[12], as it naturally retrieves the Maximum Likelihood Estimator of the Poisson distribution when focused on a single depth plane [13]. Recently, object recognition by DoP has been combined with neural networks to achieve promising results [14]. However, the capturing process for these kinds of images is relatively time-consuming and requires additional process for camera calibration. Circumventing this problem has been possible thanks to the development of plenoptic cameras [15]. Same as in Integral Imaging, a plenoptic camera can capture the light field of the scene, a recording of the irradiance as a function of both position and angular direction. The captured light field of the scene can be represented by 4D matrices. A comprehensive overview of the present Integral Imaging methods and applications can be found in [16].

Unfortunately, the performance of the detection of the DoP invariably deteriorates as the amount of light in the scene approaches photon counting levels [17]. Numerous works have analyzed the problem of determining the statistics of the DoP in the presence of Poisson noise, assuming the division operation in the DoP can be computed for all detected values of irradiance [18]–[20]. In this work we study the limits of that assumption, since under extreme low illumination environment, the sensor may not be able to detect any light at all. To do so, we further consider some simplified assumptions that (a) the sensor is ideal and only limited by Poisson noise [1] and, (b) the fluctuations in the numerator of the DoP are negligible. Using a plenoptic camera, we obtain the light fields of the scene from various perspectives under low light conditions to compute the mean value of the DoP as a function of the average number of photo detections, which is controlled by the integration (exposure) time of the sensor. The definition of the DoP is ill-suited

Manuscript received April 4, 2022; revised May 10, 2022; accepted May 11, 2022. Date of publication May 20, 2022; date of current version June 3, 2022. The work of Bahram Javidi was supported by the Air Force Office of Scientific Research under Grants FA9550-18-1-0338 and FA9550-21-1-0333, and in part by the Office of Naval Research under Grants N000141712405, N00014-17-1-2561, and N00014-20-1-2690. This work was supported by the Ministerio de Ciencia e Innovación MCIN/ AEI /10.13039/501100011033 under Grant PID2019-104268GB-C22. *(Corresponding author: Artur Carnicer.)*

Marcos Aviñoá, Salvador Bosch, and Artur Carnicer are with the Department de Física Aplicada, Universitat de Barcelona, 08007 Barcelona, Spain (e-mail: mperezavinoa@ub.edu; sbosch@ub.edu; artur.carnicer@ub.edu).

Xin Shen is with the Department of Electrical and Computer Engineering, University of Hartford, West Hartford, CT 06117 USA (e-mail: xshen@hartford.edu).

Bahram Javidi is with the Department of Electrical and Computer Engineering, University of Connecticut, Storrs, CT 06269 USA (e-mail: bahram.javidi @uconn.edu).

Digital Object Identifier 10.1109/JPHOT.2022.3176125

to deal with low detection values computationally. Fortunately, the theory does not depend on the light fields, which can be substituted by a time or multi-image averaging process over the Region of Interest (ROI). Using the theory developed in this work, we are able to correct the mean value of the detected DoP by multiplying a factor which only depends on the mean of photo detections per pixel. The commonly used denoising algorithms [11], [21] and the recently developed ones based on neural networks [22] can improve the signal-to-noise ratio (SNR) to recover the DoP. However, as we will show in this work, the value of the DoP inevitably falls to zero as the mean number of photo detections decreases. With the theory proposed in this work, we are able to boost the mean value of the DoP to keep it constant throughout different light levels, while maintaining the SNR constant.

The paper is divided as follows. First, we review some theoretical concepts used in this work. Then, we study the mean value and fluctuations of the polarized light and the total light field. We show how these two factors enter into the definition of the experimentally measured DoP, and derive a formula to predict the behavior for all possible mean number of photo detections in Appendix A. To corroborate the formulae developed in the work, experimental results are presented and analyzed. Finally, we end with some concluding remarks.

II. Review of Theoretical Concepts

A. Stokes Parameters and DoP

The DoP of light can be defined as the ratio of polarized light with respect to the total irradiance of the electromagnetic field. The Stokes parameters are usually employed to compute this value, as they provide an easy and direct way to represent the most general state of polarization of light. If $E_x,\ E_y$ are the components of an electromagnetic beam, the Stokes parameters are defined as

$$\begin{cases} S_0 = \langle E_x^\star E_x\rangle_T + \langle E_y^\star E_y\rangle_T & \text{(1a)} \\ S_1 = \langle E_x^\star E_x\rangle_T - \langle E_y^\star E_y\rangle_T & \text{(1b)} \\ S_2 = \langle E_x^\star E_y\rangle_T + \langle E_y^\star E_x\rangle_T & \text{(1c)} \\ S_3 = -i\left(\langle E_x^\star E_y\rangle_T - \langle E_y^\star E_x\rangle_T\right) & \text{(1d)} \end{cases}$$

where $\star$ denotes complex conjugation and $\langle\cdot\rangle_T$ denotes temporal averaging. Since it is rare in nature to find circularly polarized light reflected from material surfaces we assume $S_3 = 0$ throughout the article. Based on (1), the DoP is defined as

$$\text{DoP} = \frac{\sqrt{S_1^2 + S_2^2}}{S_0} = \frac{S_{\text{pol}}}{S_0}. \tag{2}$$

We have $0 \leq \text{DoP} \leq 1$, the lower bound represents unpolarized or natural light while the upper bound represents completely polarized light. Intermediate cases are collectively called partially polarized light.

This definition leads us into the interpretation of the Stokes parameters as coordinates bounded by a sphere, the PoincarÃ sphere. Representing the normalized Stokes parameters in the form $(1, S_1/S_0, S_2/S_0, 0)$, we see that the completely polarized beams represent points on the surface of the sphere, while a partially polarized light beam lies in its volume. A completely unpolarized light beam represents the particular case of the center of the sphere.

B. Light Detection

Equation (1) is defined in terms of the electromagnetic fields. However, at optical frequencies, it is not feasible to follow the variation of the fields with time. Optical sensors measure the amount of electrons which are generated by the light impinging on them, and this process is only sensitive to the irradiance of the light.

When considering either the semi-classical or fully quantum approach, the phenomenon of light detection is described as a random process with discrete values. In general, the detection probability is given by averaging a Poisson distribution over all coherent quantum states of the light $\{\Phi\}$

$$p(n,t,T) = \left\langle W\frac{\mathrm{e}^{-W}}{n!}\right\rangle_\Phi, \tag{3}$$

where t is the time variable and

$$W = \eta\int_t^{t+T} I(t')dt' \tag{4}$$

is the total number of incident photons recorded by the detector within the integration time interval T, and $I(t)$ is the incident irradiance [1]. If T is large enough, so that $T \gg \tau_c$ where τ_c is the coherence time of the light, (4) will average the fluctuations of the incident irradiance, which in turn averages the contribution of the different coherent quantum light states. In this work, since we use (i) LED sources that can be considered as quasi-thermal light and (ii) a conventional camera sensor with $T > 1$ ms, the approximation mentioned above is adequate. Thus (4) can be rewritten as $W \approx \eta T\langle I\rangle$ and the detection probability of n photons is given by

$$p(n,T) \approx \frac{(\eta T\langle I\rangle)^n}{n!}\mathrm{e}^{-\eta T\langle I\rangle}, \tag{5}$$

where η is the quantum efficiency of the detector (amount of excited electrons per incoming photon) and $\langle I\rangle$ is the averaged irradiance of light over the time interval T, in photons per second. The probability function corresponds to a Poissonian distribution with a rate parameter $\lambda = \eta T\langle I\rangle$. An interesting consequence of the light detection process is that for a continuous and complex valued signal, we can only recover a quantized version of its squared modulus: all information regarding the phase of the beam is lost in the process. We restate that (5) is derived, and thus only correct, assuming neither electronic nor bias noise is present in the detector.

III. Detection, Calculation, and Bias of the DoP

The DoP is detected through the use of the Stokes parameters as discussed in Section II-A. Experimentally, the correlations in (1) are impossible to detect due to the rapid fluctuations of the electromagnetic field. To recover those values, a setup as shown in Fig. 1 is employed. Before the camera, we place a linear

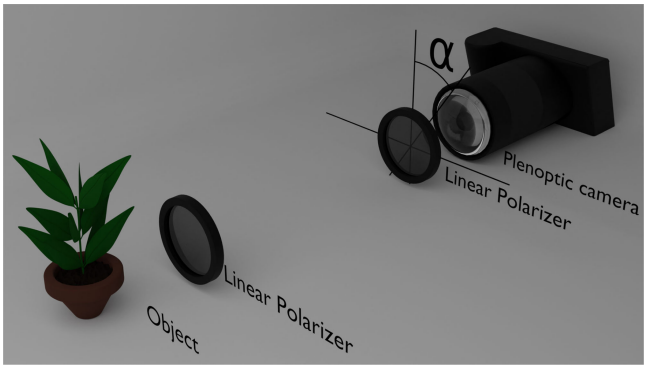

Fig. 1. Scheme of the experimental setup for capturing the light fields $L^{\{\alpha\}}$ of the scene under low light environment to retrieve the Stokes parameters.

polarizer tuned to the wavelength of the light. This polarizer constitutes a polarization state analyzer, which is capable of detecting the irradiance of a single polarization state. In this work we apply the Integral Imaging technology, the light field imaging, for 3D sensing, as it has been demonstrated that they are able to improve the detection of the DoP [10]–[12]. A plenoptic camera is used to capture the light fields in a single shot. The following set of light fields L^{α} are captured, following the polarimetric measurements presented in [3],

$$\{L^{\alpha}\} = \left\{L^{0^\circ},\, L^{45^\circ},\, L^{90^\circ},\, L^{135^\circ}\right\} \tag{6}$$

where α is the rotation angles of the linear polarizer. The Stokes parameters, defined in terms of these captured light fields, are

$$\begin{cases} S_0 = \frac{1}{2}\left(L^{0^\circ} + L^{45^\circ} + L^{90^\circ} + L^{135^\circ}\right) & \text{(7a)} \\ S_1 = L^{0^\circ} - L^{90^\circ} & \text{(7b)} \\ S_2 = L^{45^\circ} - L^{135^\circ} & \text{(7c)} \end{cases}$$

where, same as mentioned in Section II-A, we ignore the contribution of S_3 due to the fact that circularly polarized light is rare in nature.

Finally, we include a linear polarizer in front of the object to control the state of polarization of light.

As defined in (7), the DoP is a function of Poissonian random variables in the absence of external noise. Under regular illumination conditions (the mean number of photo detections is relatively high), the DoP is a well-behaved function and its computation does not present problems. Moreover, the Poissonian statistics of the pixel irradiances in the polarimetric images converge to the Gaussian statistics, and we can neglect the discrete nature of light detection.

Unfortunately, under low light conditions, the Poissonian statistics of the polarimetric images cannot be neglected. Based on the definition, (2), the DoP is a ratio of two functions: S_{pol} and S_0. Numerically, the DoP is computable no matter what the value of S_{pol} is. However, the denominator (S_0) presents a grave problem if it has a non-negligible probability of being equal to zero. In this case, irrespective of the value of the numerator, the division cannot be computed. S_0 is a Poissonian random variable because it is the sum of the independent Poissonian random variables. Indeed, from (7) we can show that

$$\begin{aligned} S_0 &= \frac{1}{2}\left[\left(L^{0^\circ} + L^{45^\circ}\right) + \left(L^{90^\circ} + L^{135^\circ}\right)\right] \\ &= \frac{1}{2}\left(L_{t1} + L_{t2}\right) \end{aligned} \tag{8}$$

where L_{ti} is a measurement of the total light field at different points in time. As the correlation time of natural light is very small, these two different total irradiances constitute independent Poissonian random variables. Consequently, depending on the mean value of photo detections, the probability of obtaining the measurement zero may not be negligible.

The problem mentioned above is usually circumvented by performing an average over different measurements of S_0, such as in [18]–[20]. The resulting mean value will also be a Poisson random variable, but with a narrower spread. Unfortunately, if the mean number of photo detections is too small or the number of S_0 samples is not sufficient, the probability that the mean value of S_0 ($\langle S_0 \rangle$) will be very small is not negligible. Furthermore, due to the potential low light measurements, the mean value of the measurements may be very close to zero as well. In turn, such measurements under the ideal noise free conditions may cause the DoP values to be higher than the unity and cannot be regarded as a correct measurement. Under real conditions, it has been reported that the computed DoP will decrease to zero along with the mean value of the photo detections which decrease to zero [17].

Under such stringent conditions, we need to completely remove the value of zero from the definition of S_0 to perform an accurate computation of the DoP. This means that the denominator effectively becomes a zero-truncated Poisson random variable, N. It can be shown that zero-truncated Poisson probability function is given by [23]

$$P(n, \langle S_0 \rangle) = \frac{\langle S_0 \rangle^n}{n!} \frac{\mathrm{e}^{-\langle S_0 \rangle}}{1 - \mathrm{e}^{-\langle S_0 \rangle}};\ n \in \mathcal{Z}^+, \tag{9}$$

where n is the random variable related with the number of photo detections with zero excluded, $\langle S_0 \rangle = \eta T \langle I \rangle$ and the brackets denote an averaging process over the angular dimensions of the light field. If we use 2D images instead of the light field images, the angular averaging can be substituted by a time averaging of multiple frame images in a Region of Interest (ROI) of the same scene. The mean value and variances are [23]

$$\langle N \rangle = \frac{\langle S_0 \rangle}{1 - \mathrm{e}^{-\langle S_0 \rangle}}, \tag{10}$$

$$\begin{aligned} \langle \Delta N^2 \rangle &= \frac{\langle S_0 \rangle + \langle S_0 \rangle^2}{1 - e^{-\langle S_0 \rangle}} - \frac{\langle S_0 \rangle^2}{(1 - e^{-\langle S_0 \rangle})^2} \\ &= \langle N \rangle \left(1 + \langle N \rangle e^{-\langle S_0 \rangle}\right). \end{aligned} \tag{11}$$

The mean value might be overestimated, with respect to the correct mean of the Poissonian distribution. In the following sections we will show how to exploit such overestimation to recover a more accurate value of the DoP.

A. First Order Approximation of the DoP

The numerator of (2) is a complicated function of Poisson random variables, and a closed analytical form for its probability density function does not exist. We can make a series expansion of a function of random variables up to the second order, provided that both the means and standard deviations are well-defined. Furthermore, we assume that the Stokes parameters $\langle S_1\rangle, \langle S_2\rangle$ are uncorrelated, as they are the linear combination of Poisson random variables taken at different times. The detailed derivation can be found in Appendix A. With this consideration in mind, the mean value of the numerator is given by

$$\langle S_{\text{pol}}\rangle \approx \langle S_{\text{p}}\rangle + \frac{1}{2}\langle S_{\text{p}}\rangle^{-3}\left[(\langle S_{\text{p}}\rangle^2 - \langle S_1\rangle^2)\langle \Delta S_1^2\rangle + (\langle S_{\text{p}}\rangle^2 - \langle S_2\rangle^2)\langle \Delta S_2^2\rangle\right] \tag{12}$$

where $\langle \Delta S_1\rangle$ and $\langle \Delta S_2\rangle$ are the variances of the Stokes parameters S_1 and S_2, respectively. $\langle S_i\rangle$ corresponds to the mean value of the i-th Stokes parameter, and

$$\langle S_{\text{p}}\rangle \equiv \left(\langle S_1\rangle^2 + \langle S_2\rangle^2\right)^{1/2} \tag{13}$$

In this work we consider one more simplified assumption: the behavior of the DoP under the extreme cases of low and high light conditions is primarily affected by the distribution of the denominator in (2). This effectively means that we are imposing the variances of the Stokes parameters to be small in comparison to their mean values that $\langle S_{\text{pol}}\rangle \approx \langle S_{\text{p}}\rangle$. The validity of this imposition will be verified in the experimental results.

Under these simplified assumptions, the mean value of the DoP over the new random variable N is approximately given by

$$\text{DoP} \approx \frac{\langle S_{\text{pol}}\rangle}{\langle N\rangle} \approx \text{DoP}_0\left(1 - \text{e}^{-\langle S_0\rangle}\right) \tag{14}$$

where we have defined

$$\text{DoP}_0 = \frac{\langle S_{\text{p}}\rangle}{\langle S_0\rangle}, \tag{15}$$

as the ideal value which we wish to measure.

Equation (14) represents a biased measurement of the DoP of light, whereas the ideal measurement is given by (15). Therefore, under the approximations mentioned above, the bias of the DoP measurement is given by,

$$\text{Bias}\left(\text{DoP}, \text{DoP}_0\right) = \text{DoP} - \text{DoP}_0 = -\text{DoP}_0\text{e}^{-\langle S_0\rangle} \tag{16}$$

which is nonzero and depends on both the ideal value of the DoP and the mean number of photo detections.

B. Variance of the Measured DoP

Under the approximations considered above and assuming that the Stokes parameters S_1 and S_2 have negligible variances, we compute the variance of the measured DoP. As the probability distribution of the reciprocal of a variable can be an exceedingly complicated function, we approximate the variance by a Taylor series around the mean value of the denominator in (10). A detailed calculation is given in Appendix B. Then, combining (31) with (10) and (11), we obtain the following result:

$$\text{Var}(\text{DoP}) \approx \frac{\langle\langle S_{\text{p}}\rangle\rangle^2}{\langle S_0\rangle^3}\left(1 - \text{e}^{-\langle S_0\rangle}\right)^3\left[1 + \frac{\langle S_0\rangle}{\text{e}^{\langle S_0\rangle - 1}}\right] \approx \frac{\text{DoP}_0^2}{\langle S_0\rangle}\left(1 - \text{e}^{-\langle S_0\rangle}\right)^3\left[1 + \frac{\langle S_0\rangle}{\text{e}^{\langle S_0\rangle - 1}}\right]. \tag{17}$$

The behavior of this variance as a function of the mean number of photo detections is presented in Fig. 2 as the blue curve. We observe that with the increase of the mean of the photo detections, $\langle S_0\rangle$, the variance of the measured DoP, Var(DoP), slowly approaches to zero from its maximum point. In the opposite direction, Var(DoP) will reach to zero along with the decrease of $\langle S_0\rangle$, This can be corroborated by studying the limiting behavior of (17) as $\langle S_0\rangle \to 0$,

$$\text{Var}(\text{DoP}) \to \frac{\text{DoP}_0^2}{2}\langle S_0\rangle^2, \tag{18}$$

which indicates that Var(DoP) will quadratically decrease to zero as $\langle S_0\rangle$ approaches zero. On the other hand, if we keep the zero photo detections inside the denominator of the DoP, with the decrease of $\langle S_0\rangle$, the corresponding variance of the measured DoP will diverge, as the orange curve shown in Fig. 2.

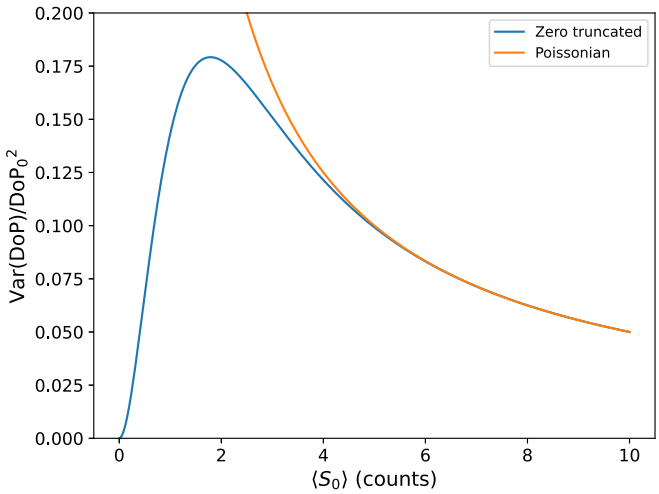

Fig. 2. The normalized variance of the measured DoP, as a function of the mean number of photo detections $\langle S_0\rangle$ divided by the square of the ideal DoP, DoP_0. (i) Blue curve: with zero truncated to the DoP. Var(DoP) converges to zero as $\langle S_0\rangle$ approaches to zero. With the increase of $\langle S_0\rangle$, Var(DoP) will first increase in a quadratic manner to a maximum, then decrease to zero again. (ii) Orange curve: without removing zero. Var(DoP) diverges as $\langle S_0\rangle \to 0$. With the increase of $\langle S_0\rangle$, it converges with the zero truncated statistics and steadily decreases to zero.

C. Numerical Simulation of the Measured DoP

To study the accuracy of the mean and variance of the measured DoP, we performed a simple simulation for the DoP of a linearly polarized beam, whose Stokes parameters are $S_0 = S_2$ and zero for the rest. Under the approximations considered in the previous sections, both the numerator and denominator of the DoP will follow the Poisson statistics. In our work, 100 random values for different mean numbers of photo detections are generated for both the numerator and denominator. Note

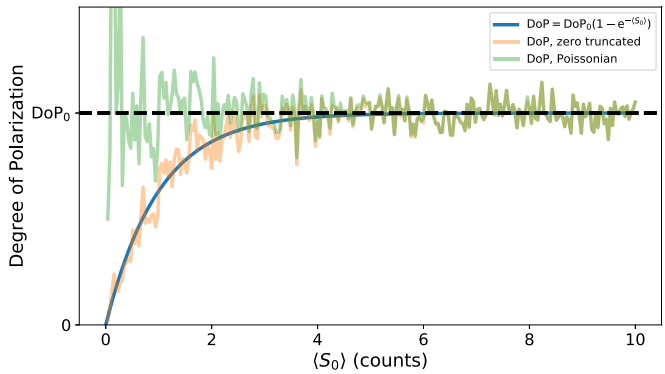

Fig. 3. Dependence of the DoP as a function of the mean value of the Stokes parameter S_0. The blue curve is based on Eq. (14), the orange curve is the simulation of the computed DoP using zero truncated Poisson statistics in the denominator, and the green curve represents the computed DoP under full Poisson statistics including zeros.

that, we perform the average on the numerator and denominator separately before the division between them.

We first analyze the effect by removing all zeros (zero truncated) before the averaging of the denominator. The corresponding behavior is represented by the orange curve in Fig. 3 The blue curve corresponds to the approximation of the mean value of the DoP described by (14). As shown in Fig. 3, both the orange and blue curves indicate a decrease of the DoP under extremely low illumination conditions, and a saturation to a constant value for moderately higher photo detections. In low illumination conditions, the DoP is seen to be linearly proportional to the total incident irradiance in the scene, given by $\langle S_0 \rangle$. Taking the limit of $\langle S_0 \rangle \to 0$ in (14) results in

$$\text{DoP} \approx \text{DoP}_0 \langle S_0 \rangle. \tag{19}$$

Due to this linearity, we expect that noise will play a significant role in the retrieval of the DoP under the extreme case of photon starvation. Moreover, the variance of the measured DoP in the orange curve of Fig. 3 decreases as the mean number of photo detections approaches to zero. This matches with the predicted result of (18).

A simulation of the DoP using full Poissonian statistics and maintaining all zeros before averaging is represented by the green line in Fig. 3. Under high illumination conditions, both the zero truncated and Poissonian statistics coincide in the mean value. The bias introduced by the zero truncated Poisson distribution is negligible under such conditions. However, for very small mean numbers of photo detections, the measured DoP without the zero maintains a mean value which is close to the ideal one, but with extremely high oscillations.

As shown in Fig. 3, the zero truncated Poisson distribution approach presented in this work allows for a less noisy computation of the DoP, and the simulated results fit very well with the first order approximation of (14). In the following sections, we will apply this approach to recover a better estimation of DoP under low illumination conditions. Note that, (19) indicates that under very poor illumination conditions the computed DoP reduces to zero independently of the polarization state of light, so that we can not retrieve the DoP of the light.

IV. Experimental Results and Discussions

The experimental setup consists of a polarizer with its axis at 45° with respect to the y direction illuminated by a red LED light, a plenoptic camera and a linear polarizer. The plenoptic camera used is a Lytro Illum, with a constant 3200 ISO sensitivity. Eight different series of polarimetric images have been taken, with respective integration times, $T = 0.0125, 0.025, 0.1, 0.156, 0.25, 0.5, 1, 2$ s. For each integration time, the read noise is estimated by averaging ten different light fields captured in complete darkness. This estimation is then subtracted from each polarimetric image. In this work, we use the light field imaging, as its superiority over conventional imaging under low light conditions has been demonstrated [13].

The scene consists of a linear polarizer with a constant, featureless background. The focal plane of the irradiance after the angular averaging of light fields is at the depth plane of the polarizer. The illumination is constant throughout the experiment, with a red LED lamp. To obtain better statistics on the measured DoPs, we perform an average over a ROI in addition to the angular average of the Stokes parameters (due to the use of light fields in this work). As shown in Fig. 4(a), the polarizer is mostly a uniform surface. The total irradiance of the polarimetric images, S_0, for the highest integration time, is presented in Fig. 4(b).

The most strict assumption in this work is the fluctuations in (14) need to be small in comparison to the mean value. We divided the Stokes parameter S_2 by its mean value for various integration times and plot the histogram as shown in Fig. 5. We select S_2 because it represents the amount of light that is polarized at $\pm 45^\circ$, which is the angle between the axis of the polarizer and the horizontal plane.

Fig. 5 indicates that the relative width of the distributions with respect to their mean remain narrow, except for the lowest two integration times (0.025 s and 0.0125 s). The DoPs in these two conditions are very close to zero, as seen in Fig. 6, which shows that the exponential term in (14) dominates even under low illumination conditions.

Experimental results of the recovered DoPs corresponding to various integration times are presented in Fig. 6(a), where the dots correspond to the measured points in the experiment, and the dashed line corresponds to the experimental fit of the points following (14), in the form

$$\text{DoP} = C_0(1 - \mathrm{e}^{-C_1 T}). \tag{20}$$

By means of the Least Squares method, we obtained the best fit to the parameters of this equation using the experimental data in Fig. 6

$$C_0 = 0.659 \tag{21}$$

$$C_1 = 8.368 s^{-1} \tag{22}$$

The first parameter, C_0, corresponds to the ideal DoP in the ROI. The second parameter, C_1, contains the information about the

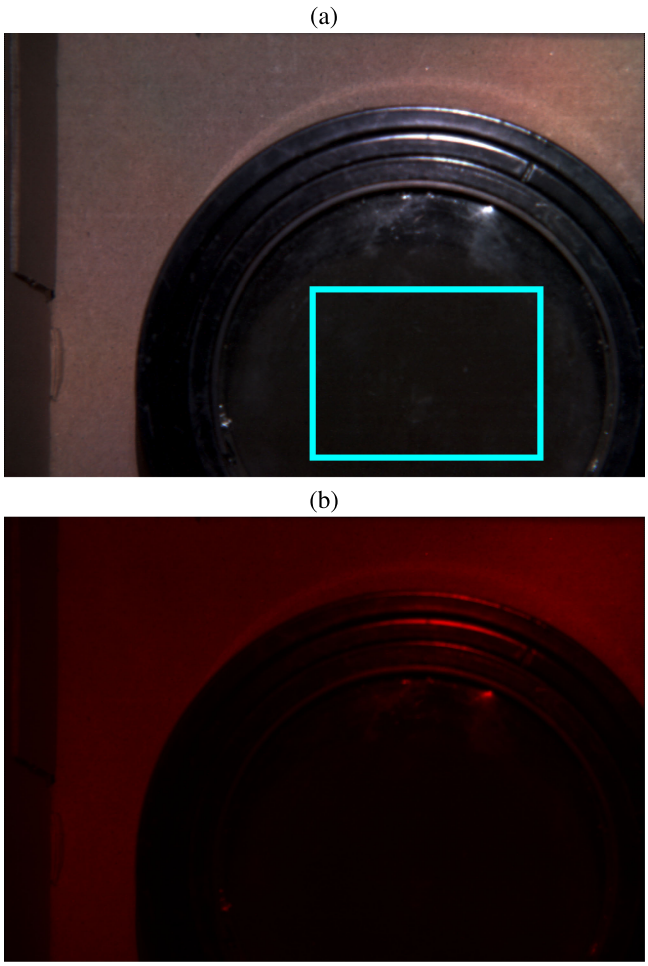

Fig. 4. Polarizer used in the experimental measurements under (a) full illumination with the ROI highlighted and (b) S_0 of the experimental scene after angular summation. The illuminating light is a red LED under a constant irradiance throughout the experiment.

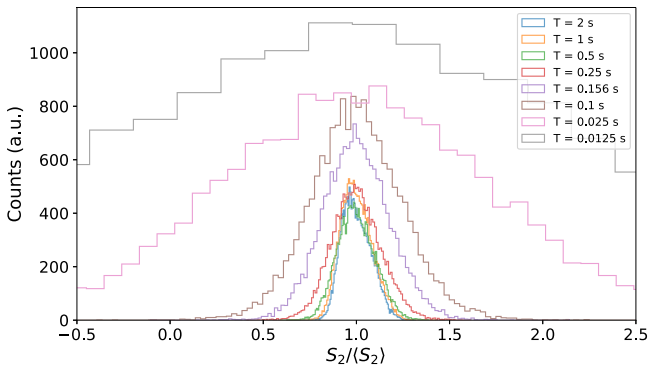

Fig. 5. The histograms for the Stokes parameter S_2 divided by their mean value within eight different integration times.

mean number of photons and quantum efficiency of the sensor. We observe an overall agreement between experiment and theory. For short integration times, the estimated DoP linearly decreases to zero, while for longer integration times, the DoP reaches a saturation value. For the moderately short integration times, the measured values are lower than the expected values

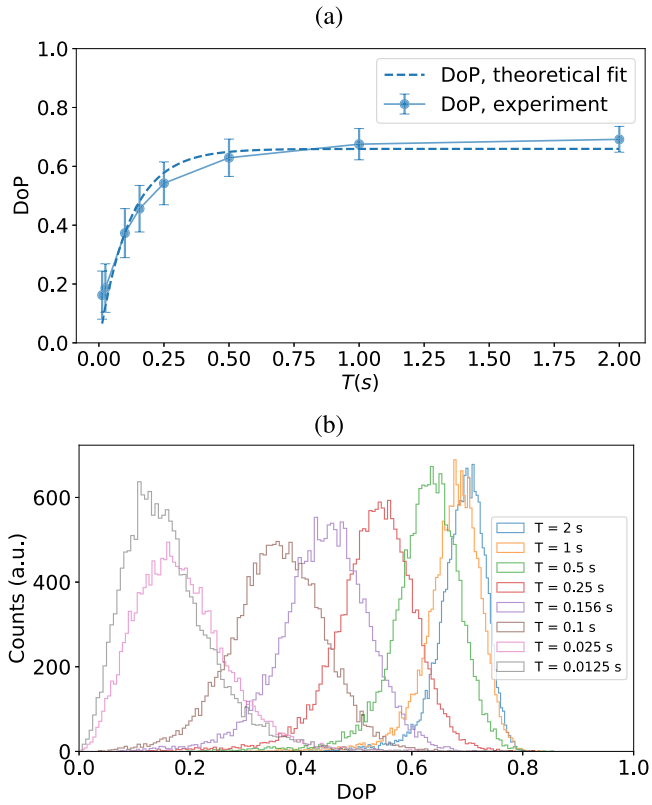

Fig. 6. (a) Variation of the mean values of the DoP as a function of the integration time of the camera, and (b) distribution of the DoP values along the ROI for the different integration times.

according to (14). This could be caused by the existence of a residual signal dependent noise, which can not be completely eliminated. Fig. 6(b) shows the histograms of the DoP in the ROI. We observe the steady decrease of its mean value and a widening of its distribution as the integration time (T) decreases, as well as the reduction of its symmetry. With our approach, the measurement error for the computation of the DoP is almost a constant.

Using value C_1 (22), we are able to correct the detected DoP from the polarimetric images as a function of the integration time, and obtain the corrected DoP (DoP_{corr}) using (20),

$$\text{DoP}_{\text{corr}}(T) = \frac{\text{DoP}(T)}{1 - \text{e}^{-C_1 T}}. \tag{23}$$

where $\text{DoP}(T)$ is the computed value of the DoP using (2). We need to resort to this approach because the information captured by the image sensor is not enough, and it is difficult to measure the average number of photons from the scene. As shown in Fig. 7(b), under low illumination conditions, the DoP results (DoP_{corr}) based on the proposed method remain as a constant with the decrease of integration time, which corresponds to the decrease of the number of the detected photons, note that, exceptional cases exist for the lowest integration times $T = 0.025$ s and

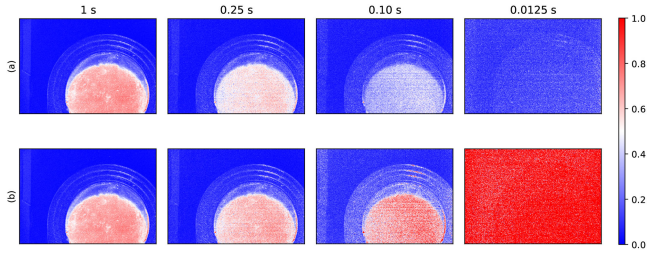

Fig. 7. Experimental results of the polarimetric imaging of the scene. (a) The DoP images by using the conventional approach, (b) Corrected DoP images based on (23). The proposed method can improve the DoP and retain the correct information under low light environments, except for extreme low illumination conditions where the sensor noise completely obscures the signal.

$T = 0.0125$ s, In these conditions, the signal is too weak comparing with the noise level, so that the values of DoP_{corr} are saturated and much higher than the unity.

This fact can be attributed to two main factors. The first one is that under very low light conditions, the decay is approximately linear and proportional to the total amount of light in the scene, as shown in (19). The measurements of S_0 become riddled with Poissonian noise, which will reduce the accuracy of the reconstruction of (23). The second factor is the increase of sensor noise with respect to light signal. As shown in Fig. 7, $T = 0.0125$ s, the corresponding DoP images have higher noise level. As we discussed before, this perturbs the corrections and makes it impossible to recover the mean value of the DoP. This is because under extreme low integration times, the denominator in (23), becomes very small, and it will corrupt the corrected value if the experimental DoP does not follow the approximation in (14). In our experiment, the noise level of the Lytro Illum camera sensor is relatively high comparing with the low integration times ($T = 0.025$ s and $T = 0.0125$ s), and the noise can not be eliminated by the subtraction of its mean value.

V. Conclusion

Under thermal light and high integration times, light detection is a Poisson random process. Under low illumination conditions, with the decrease of the mean number of photo detections, the probability of detecting few to no photons becomes non-negligible. When computing the DoP, this presents a practical computational problem, that is, we cannot divide a numerator by zero or any small value as it may cause the DoP to be non-computable. To circumvent this problem, an approach is proposed to exclude the zeros from the denominator of the DoP. This changes the distribution of the photon detection from Poisson to a truncated Poisson distribution. With this approach, we have shown that the mean value of the DoP matrix decreases to zero predictably as the mean number of photo detections approaches zero, which is independent of the state of the polarization of light.

In the experiments, we applied 3D light field for polarimetric imaging under low illumination environments to verify the proposed approach. The experimental results of the estimated DoPs fit well with the theoretical analysis. We are able to correct the measurements and maintain the accurate mean value of the DoPs for various short integration time periods. The proposed approach is limited when the integration time gets very small, which presents extremely low illumination conditions. In this case, the unaccounted noise on captured light (S_0) will make the recovery of DoP impossible. A correction can be applied if priors are obtained, that is, the characteristics of the image sensor and the average number of detected photons are known.

Appendix A
Approximation to the Mean Value of a Function of Random Variables

Since the Stokes parameters enter the DoP as the square root of the sum of their squares, their probability distribution becomes an exceedingly complicated function without a closed analytic form. To obtain a significant result, we approximate the value of $S_{\text{pol}}(S_1, S_2)$ in a Taylor series around $(\langle S_1\rangle, \langle S_2\rangle)$. To make the derivation clearer, we consider the expansion of the function

$$f(x,y) = \left(x^2 + y^2\right)^{1/2} \tag{24}$$

around (x_0, y_0). Up to second order, the Taylor series expansion is given by

$$\begin{aligned} f(x,y) \approx f(x_0,y_0) + \sum_i \left(\frac{\partial f}{\partial x_i}\right)_{x_0,y_0} (x_i - x_{i0}) + \\ + \frac{1}{2}\sum_i \left(\frac{\partial^2 f}{\partial x_i^2}\right)_{x_0,y_0} (x_i - x_{i0})^2 + \\ \sum_i \sum_{j\neq u} \left(\frac{\partial^2 f}{\partial x_i \partial x_j}\right)_{x_0,y_0} (x_i - x_{i0})(x_j - x_{j0}), \end{aligned} \tag{25}$$

where $x_i = x, y$. Now the values x_0, y_0 are considered to be the mean values of x, y respectively, in a statistical sense, and it is further assumed that the variables x, y are not correlated. On computing the mean value of (25) only the constant and non-crossed quadratic terms will survive:

$$\langle f(x,y)\rangle \approx (x_0^2 + y_0^2)^{1/2} + \frac{1}{2}\sum_i \left(\frac{\partial^2 f}{\partial x_i^2}\right)_{x_0,y_0} \langle \Delta x_i^2\rangle \tag{26}$$

which is just a correction of $f(\cdot)$ as a function of the mean values and the variances of the random variables it depends on. Substituting $f \to S_{\text{pol}}$, $x_i \to S_i$ we obtain

$$\begin{cases} \langle S_{\text{p}}\rangle \equiv \left(\langle S_1\rangle^2 + \langle S_2\rangle^2\right)^{1/2} & \text{(27a)} \\ \langle S_{\text{pol}}\rangle \approx \langle S_{\text{p}}\rangle + \frac{1}{2}\langle S_{\text{p}}\rangle^{-3} \\ \qquad \times \left[(\langle S_{\text{p}}\rangle^2 - \langle S_1\rangle^2)\langle \Delta S_1^2\rangle \right. \\ \qquad \left. + (\langle S_{\text{p}}\rangle^2 - \langle S_2\rangle^2)\langle \Delta S_2^2\rangle\right] & \text{(27b)} \end{cases}$$

where $\langle S_i\rangle$ corresponds to the mean value of the ith Stokes parameter.

Appendix B
Variance of a Reciprocal Random Variable

The variance of the reciprocal of a random variable y requires, in general, the computation of $\langle y^{-1}\rangle$ and $\langle y^{-2}\rangle$, which may be difficult to prove analytically. In this work, we are going to study an approximation to this value by developing the reciprocal

function around the mean of the random variable, similarly as performed in Appendix A. The Taylor series of the reciprocal function, up to the second order, is given by

$$\frac{1}{y} \approx \frac{1}{\langle y \rangle} - \frac{y - \langle y \rangle}{\langle y \rangle^2} + \frac{(y - \langle y \rangle)^2}{\langle y \rangle^3}, \tag{28}$$

while for the square of the reciprocal, it is given by

$$\frac{1}{y^2} \approx \frac{1}{\langle y \rangle^2} - 2\frac{y - \langle y \rangle}{\langle y \rangle^3} + 3\frac{(y - \langle y \rangle)^2}{\langle y \rangle^4} \tag{29}$$

Taking the mean value of both sides, we get the following results

$$\begin{cases} \left\langle \frac{1}{y} \right\rangle \approx \frac{1}{\langle y \rangle} + \frac{\langle \Delta y^2 \rangle}{\langle y \rangle^3} & \text{(30a)} \\ \left\langle \frac{1}{y^2} \right\rangle \approx \frac{1}{\langle y \rangle^2} + 3\frac{\langle \Delta y^2 \rangle}{\langle y \rangle^4} & \text{(30b)} \end{cases}$$

where $\langle \Delta y^2 \rangle$ is the variance of the random variable y. Combining these two equations, the variance of the reciprocal function is given by:

$$\left\langle \Delta \left(\frac{1}{y} \right)^2 \right\rangle \approx \frac{\langle \Delta y^2 \rangle}{\langle y \rangle^4} - \frac{\langle \Delta y^2 \rangle^2}{\langle y \rangle^6} \approx \frac{\langle \Delta y^2 \rangle}{\langle y \rangle^4}, \tag{31}$$

where high order contributions to the variance of y are ignored.

ACKNOWLEDGMENT

The authors would like to thank Gokul Krishnan and Kashif Usmani for their insightful remarks.

REFERENCES

[1] L. Mandel and E. Wolf, *Optical Coherence and Quantum Optics*, 1st ed., Cambridge, UK: Cambridge Univ. Press, 1995.
[2] J. Goodman, *Introduction to Fourier Optics*. Calgary, Canada: Roberts & Company, 2005.
[3] M. Born and E. Wolf, *Principles of Optics: Electromagnetic Theory of Propagation, Interference and Diffraction of Light*. Cambridge, U.K: Cambridge Univ. Press, 1999.
[4] K. E. Torrance and E. M. Sparrow, "Theory for off-specular reflection from roughened surfaces," *J. Opt. Soc. Amer.*, vol. 57, pp. 1105–1114, Sep. 1967.
[5] L. B. Wolff, "Polarization vision: A new sensory approach to image understanding," *Image Vis. Comput.*, vol. 15, no. 2, pp. 81–93, 1997.
[6] P. Miche, A. Bensrhair, and D. Lebrun, "Passive 3-D shape recovery of unknown objects using cooperative polarimetric and radiometric stereo vision processes," *Opt. Eng.*, vol. 44, no. 2, pp. 1–9, 2005.
[7] F. A. Sadjadi, "Passive three-dimensional imaging using polarimetric diversity," *Opt. Lett.*, vol. 32, pp. 229–231, Feb. 2007.
[8] G. Lippman, "Reversible tests giving a sensation of relief," (in French), *J. Phys. Theor. Appl*, vol. 7, no. 1, pp. 821–825, 1908.
[9] M. Martínez-Corral and B. Javidi, "Fundamentals of 3D imaging and displays: A tutorial on integral imaging, light-field, and plenoptic systems," *Adv. Opt. Photon.*, vol. 10, pp. 512–566, Sep. 2018.
[10] X. Xiao, B. Javidi, G. Saavedra, M. Eismann, and M. Martinez-Corral, "Three-dimensional polarimetric computational integral imaging," *Opt. Exp.*, vol. 20, pp. 15481–15488, Jul. 2012.
[11] A. Carnicer and B. Javidi, "Polarimetric 3D integral imaging in photon-starved conditions," *Opt. Exp.*, vol. 23, pp. 6408–6417, Mar. 2015.
[12] K. Usmani, X. Shen, T. O'Connor, and B. Javidi, "Overview of three-dimensional polarimetric imaging in photon starved conditions," in *Proc. Imag. Appl. Opt. Congr.*, OSA Tech. Digest (Optica Publishing Group), 2020, PaperDTh3A.3.
[13] B. Tavakoli, B. Javidi, and E. Watson, "Three dimensional visualization by photon counting computational integral imaging," *Opt. Exp.*, vol. 16, pp. 4426–4436, Mar. 2008.
[14] K. Usmani, G. Krishnan, T. O'Connor, and B. Javidi, "Deep learning polarimetric three-dimensional integral imaging object recognition in adverse environmental conditions," *Opt. Exp.*, vol. 29, pp. 12215–12228, Apr. 2021.
[15] R. Ng, M. Levoy, M. Brédif, G. Duval, M. Horowitz, and P. Hanrahan, "Light field photography with a hand-held plenoptic camera," Tech. Rep. CTSR 2005-02, Stanford Univ., Stanford, CA, USA, 2005.
[16] B. Javidi *et al.*, "Roadmap on 3D integral imaging: Sensing, processing, and display," *Opt. Exp.*, vol. 28, pp. 32266–32293, Oct. 2020.
[17] X. Shen, A. Carnicer, and B. Javidi, "Three-dimensional polarimetric integral imaging under low illumination conditions," *Opt. Lett.*, vol. 44, pp. 3230–3233, Jul. 2019.
[18] N. Hagen, "Statistics of normalized stokes polarization parameters," *Appl. Opt.*, vol. 57, pp. 5356–5363, Jul. 2018.
[19] J. Dai, F. Goudail, M. Boffety, and J. Gao, "Estimation precision of full polarimetric parameters in the presence of additive and poisson noise," *Opt. Exp.*, vol. 26, pp. 34081–34093, Dec. 2018.
[20] J. Dai and F. Goudail, "On the validity domain of approximations to estimation variance of polarization degree, azimuth, and ellipticity," *J. Opt. Soc. Amer. A*, vol. 36, pp. 1295–1305, Aug. 2019.
[21] A. Carnicer, S. Bosch, and B. Javidi, "Mueller matrix polarimetry with 3D integral imaging," *Opt. Exp.*, vol. 27, pp. 11525–11536, Apr. 2019.
[22] X. Li *et al.*, "Learning-based denoising for polarimetric images," *Opt. Exp.*, vol. 28, pp. 16309–16321, May 2020.
[23] N. Johnson, S. Kotz, and A. Kemp, *Univariate Discrete Distributions*. Hoboken, NJ, USA: Wiley, 1992.